



**HAL**  
open science

## Deep Level Transient Fourier Spectroscopy (DLTFS) and Isothermal Transient Spectroscopy (ITS) in vertical GaN-on-GaN Schottky barrier diodes

P. Vigneshwara Raja, Christophe Raynaud, Camille Sonnevile, Hervé Morel,  
Luong Viet Phung, Thi Huong Ngo, Philippe de Mierry, Eric Frayssinet,  
Hassan Maher, Yvon Cordier, et al.

### ► To cite this version:

P. Vigneshwara Raja, Christophe Raynaud, Camille Sonnevile, Hervé Morel, Luong Viet Phung, et al.. Deep Level Transient Fourier Spectroscopy (DLTFS) and Isothermal Transient Spectroscopy (ITS) in vertical GaN-on-GaN Schottky barrier diodes. *Micro and Nanostructures*, 2022, 172, pp.207433. 10.1016/j.micrna.2022.207433 . hal-04032160

**HAL Id: hal-04032160**

**<https://hal.science/hal-04032160>**

Submitted on 16 Mar 2023

**HAL** is a multi-disciplinary open access archive for the deposit and dissemination of scientific research documents, whether they are published or not. The documents may come from teaching and research institutions in France or abroad, or from public or private research centers.

L'archive ouverte pluridisciplinaire **HAL**, est destinée au dépôt et à la diffusion de documents scientifiques de niveau recherche, publiés ou non, émanant des établissements d'enseignement et de recherche français ou étrangers, des laboratoires publics ou privés.

# Deep Level Transient Fourier Spectroscopy (DLTFS) and Isothermal Transient Spectroscopy (ITS) in Vertical GaN-on-GaN Schottky Barrier Diodes

P. Vigneshwara Raja<sup>a,b\*</sup>, Christophe Raynaud<sup>b</sup>, Camille Sonnevill<sup>b</sup>, Hervé Morel<sup>b</sup>, Luong Viet Phung<sup>b</sup>, Thi Huong Ngo<sup>c</sup>, Philippe De Mierry<sup>c</sup>, Eric Frayssinet<sup>c</sup>, Hassan Maher<sup>d</sup>, Yvon Cordier<sup>c</sup> and Dominique Planson<sup>b</sup>

<sup>a</sup>Department of Electrical Engineering, Indian Institute of Technology (IIT) Dharwad, Karnataka - 580011, India.

<sup>b</sup>Univ. Lyon, INSA Lyon, Univ. Claude Bernard Lyon 1, Ecole Centrale Lyon, CNRS, Ampère, Villeurbanne Cedex F-69621, France.

<sup>c</sup>Université Côte d'Azur, CNRS, CRHEA, Valbonne 06560, France.

<sup>d</sup>Université de Sherbrooke, CNRS-UMI\_LN2, Sherbrooke, Quebec J1K 2R1, Canada.

\*E-mail: vigneshwararaja@iitdh.ac.in

## Abstract:

The paper explores the Deep Level Transient Fourier Spectroscopy (DLTFS) capabilities in characterizing electrically active traps in vertical GaN-on-GaN Schottky barrier diodes (SBDs). The capacitance-DLTFS (C-DLTFS) experiments reveal a prominent electron trap T2 at  $E_C - 0.56$  eV with a density ( $N_{T2}$ ) of  $8 \times 10^{14}$  cm<sup>-3</sup> and a weak presence of another trap at  $E_C - 0.18$  eV (T1) with  $N_{T1} = 3.8 \times 10^{13}$  cm<sup>-3</sup> in the SBDs. The C-DLTFS acquired with two emission transients ( $T_E = 20.48$  ms and 2.048 s) has resulted in identical trap signatures for T1 and T2. Due to the high  $N_T$ , the trap T2 at  $E_C - 0.56$  eV is identified from the current-DLTFS (I-DLTFS) and thermally stimulated capacitance (TSCAP) measurements. Especially the TSCAP results indicate the carrier freeze-out temperature ( $T < 75$  K) in the GaN material. Furthermore, the carrier emission kinetics of the trap T2 is evaluated by performing isothermal transient spectroscopy at a stabilized temperature. The capture time constant of T2 is estimated from the isothermal transients attained with shorter trap-filling pulse widths ( $< 100$  ns).

**Keywords:** Free-standing GaN, Schottky barrier diode, DLTFS, traps, capacitance and current DLTS, Isothermal transient.

## 1. Introduction

The availability of free-standing GaN substrate (GaN-on-GaN structure) has opened a doorway in manufacturing vertical power devices with the absence of lattice and thermal expansion coefficient mismatching, mitigated dislocation density ( $< 10^7$  cm<sup>-2</sup>) in the drift layer, and device scalability [1-4]. Although the dislocation density is considerably reduced in the homoepitaxial GaN substrates, the material quality is not yet matured up to an industry-standard, due to the presence of native point defects, threading dislocations, extended defects, defect clusters, pits, and residual impurities. The crystal defects and impurities introduce electrically active traps inside the bandgap of GaN and disturb the electrical characteristics of the device through the charge trapping/detrapping phenomena. Deep level

transient spectroscopy (DLTS) is a powerful and well-established technique to identify the deep levels in semiconductor devices [5-7]. The fabrication of Schottky barrier diode (SBD) structure is relatively simple, so the metal/semiconductor junction device has been extensively used for the DLTS characterizations. The defect states can introduce additional leakage current paths in the SBD structure, as a result, reverse leakage current increases, and the breakdown voltage decreases [1,2]. During the forward bias operation, the defects can decrease the carrier mobility through scattering mechanism [6,7], thereby reducing the ON-state current and increasing the ON-resistance of the SBD. In this way, the trapping effects can induce long-term reliability issues in the GaN SBDs; thus the trap characterization experiments require special attention at the moment.

Several authors used the conventional deep level transient spectroscopy (DLTS) to identify the electrically active traps in vertical GaN-on-GaN SBDs [8-16]. The boxcar (rate-window concept) and lock-in (square wave weighting function) methods were used to compute the trap parameters through maximum temperature analysis of the DLTS curve [5-7]. However, these classical DLTS techniques are ineffective in resolving overlapping emissions resulting from the closely located trap energies, and the traps having identical emission rates [7,17]. The well-refined variant of the DLTS technique, namely deep level transient Fourier spectroscopy (DLTFS) [7,17,18] offers the following advantages: direct extraction of the trap parameters from the transient signals, improved sensitivity for characterizing traps, good noise suppression, and the possibility of tracking overlapping emission rates. So, a single thermal scan is sufficient to extract the trap parameters (activation energy, capture cross-section, and trap density) from the Arrhenius plot. Moreover, the Fourier transform-based Isothermal Transient Spectroscopy (ITS) [18] measurements can inspect the overlapping emission behaviour of the traps. The DLTFS methods were applied to detect traps in the GaN pn diodes [19,20] and AlGaIn/GaN heterostructure devices [21,22]. Muret *et al.* [23] identified deep level trap energies ranging from 0.94eV to 1.3 eV in n-type GaN films by Fourier transform DLTS (FTDLTS) procedure. Therefore, very few reports are available in the literature on the DLTFS characterization of vertical GaN-on-GaN SBDs. Since the GaN material quality keeps improving, it is essential to acquire the quantitative information of the traps present in the vertical GaN-on-GaN SBDs.

This study uses the DLTFS method [17] to characterize traps in the SBDs fabricated on Si-doped n-type homoepitaxial GaN layers. For this purpose, capacitance- and current-mode DLTFS (C-DLTFS and I-DLTFS) [17,18] characterizations are carried out in the temperature range of 20 K to 460 K. Thermally stimulated capacitance (TSCAP) [24-27] spectroscopy measurements are performed to complement the DLTFS results. The carrier capture and emission kinetics are evaluated by conducting isothermal transient spectroscopy (ITS) [13] at a stabilized temperature. Therefore, the trap characterization capabilities of the DLTFS technique are well explored for the vertical GaN-on-GaN SBDs. This work is intended to provide complete information of traps in the n-type homoepitaxial GaN substrates. So, the current work results can benefit the material science community in optimizing the GaN growth process technology.

## 2. DLTS Technique

### 2.1. Fundamentals of DLTS

In DLTS [5-7,18,24,26], the traps in the device are alternatively filled and emptied by the voltage pulsing procedure. The capacitance or current transient signal is recorded during the detrapping process. For instance, a single electron trap at  $E_C - E_T$  is considered in the n-type GaN SBD. Initially, the SBD is kept under quiescent reverse bias ( $V_{QR}$ ), so the traps inside the space charge region (SCR) have a small probability of capturing electrons due to the lack of free electrons in the conduction band. The charge state of the trap and the energy band diagram at  $V_{QR}$  are shown in Fig.1. The trap-filling pulsing scheme employed in this work is depicted in Fig. 2(a). The reduced reverse bias pulse ( $V_P$  close to zero voltage) momentarily introduces majority carriers (electrons in n-type semiconductor) in the region previously the part of the SCR. At this instant, if the trap energy  $E_T$  goes below the Fermi level, they can capture the electrons in the region. If the capture process follows a typical exponential behaviour, the respective increase in the trapped electrons ( $n_{Tc}$ ) during the capture transient ( $t_P$ ) can be expressed as [6,7,18,24,26]

$$n_{Tc}(t) = N_T(1 - \exp(-t/\tau_c)) \quad (1)$$

where  $N_T$  is the trap concentration. The capture time constant ( $\tau_c$ ) is given by

$$\tau_c = 1/c_n = 1/\sigma_n v_{th} n \quad (2)$$

where  $c_n$  is the capture rate,  $\sigma_n$  is the capture cross-section, and  $n$  is the free-electron concentration. Once the pulse returns to its quiescent reverse bias ( $V_{QR}$ ), a rapid drop in the capacitance is noticed in Fig. 2(b) due to the fast sweep-out of free carriers in the re-established SCR region. At this point, the trapped electrons ( $n_{Tc}$ ) in the SCR compensate part of the ionized donors [7, 24-27], so that the effective junction capacitance ( $C_R$ ) reduces after the end of the filling pulse [25]

$$C_R(t) = A \sqrt{\frac{q\epsilon(N_D^+ - n_{Tc})}{2(V_R + V_{bi})}} \quad (3)$$

where  $N_D^+$  is the ionized donor concentration,  $A$  is the diode active area,  $q$  is the elementary charge, and  $V_{bi}$  is the built-in voltage of the SBD. If the trapped electrons gain sufficient thermal energy ( $E_a > E_C - E_T$ ), they are emitted from the trap level to the conduction band and subsequently swept out by the applied electric field. This thermally-activated detrapping process is seen as slowly rising capacitance transients in Fig. 2(b). The thermal emission rate ( $e_n$ ) is related to the trap energy ( $E_T$ ) by [7,18,24]

$$e_n = \frac{\sigma_n v_{th} N_C}{g} \exp\left(-\frac{E_C - E_T}{kT}\right) = 1/\tau_e \quad (4)$$

If the emission rate follows the exponential decay function, the corresponding reduction in the trapped electron density ( $n_{Te}$ ) during emission transient ( $T_E$ ) can be symbolized as [18]

$$n_{Te}(t) = N_T \exp(-t/\tau_e) \quad (5)$$

where the emission time constant ( $\tau_e$ ) is an inverse of the emission rate ( $e_n$ ). Figure 2 shows that the electron detrapping in the n-type GaN SBD induces an increasing capacitance transient during the

emission time ( $T_E$ ). On the other hand, if a hole trap exists in the n-type GaN SBD, it may produce a decreasing capacitance transient during  $T_E$ . The transient signal data is acquired at regular intervals during the thermal scan. The transient data analysis is accomplished using the DLTFs technique.

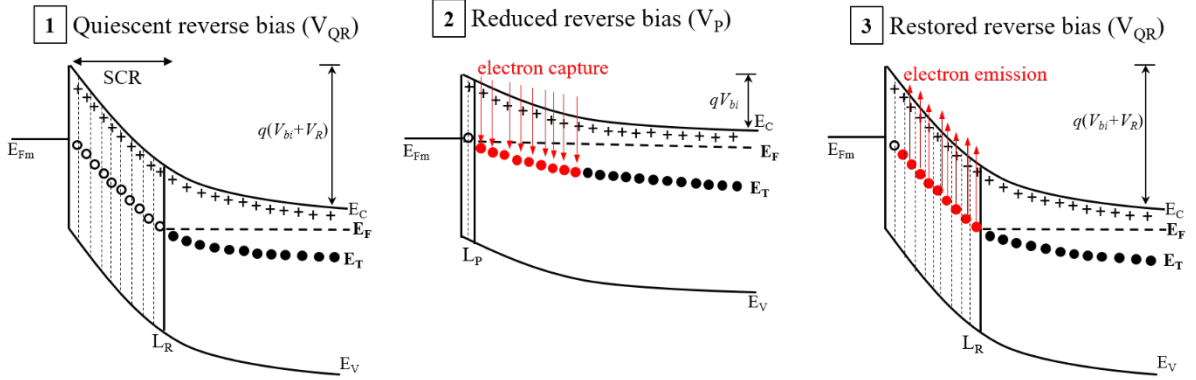


Fig. 1. Variations in energy band diagram (not to scale) and charge state of the traps under (1) quiescent reverse bias  $V_{QR}$ , (2) reduced reverse bias pulse  $V_P$  and (3) restored reverse bias  $V_{QR}$  conditions [5-7,18,24,26].

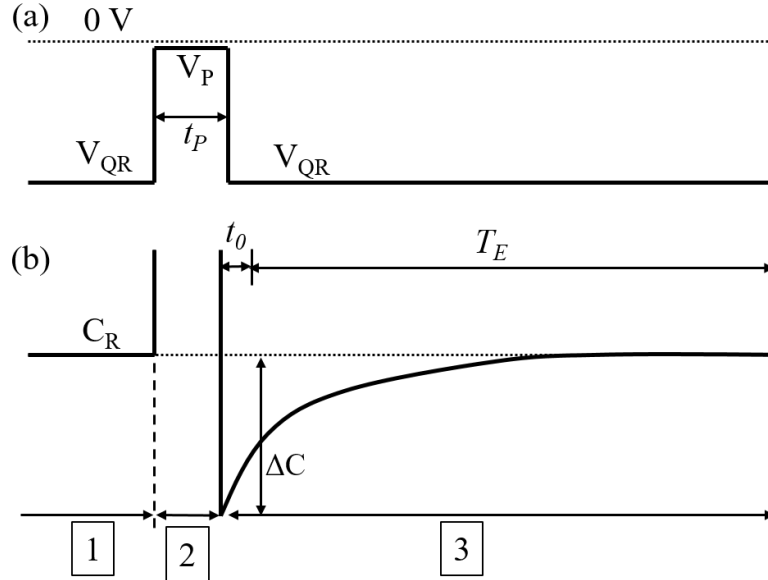


Fig. 2. (a) Reduced reverse bias pulse to fill the majority carrier (electron) traps in the n-type SBD during DLTFs characterization and (b) Resultant transient capacitance signal during the emission process [18].

## 2.2. Principle of DLTFs

The DLTFs technique first converts the transient signals into digital transients. Then numerical Fourier transformation is applied to represent the transient signal in terms of Fourier series (infinite sum of sine and cosine functions) [7,17,18]:

$$f(t) = \frac{a_0}{2} + \sum_{n=1}^{\infty} a_n \cos(n\omega t) + \sum_{n=1}^{\infty} b_n \sin(n\omega t) \quad (6)$$

where  $f(t)$  is the continuous-time signal,  $\omega = 2\pi/T_E$  is the fundamental frequency of the periodic signal,  $a_0$ ,  $a_n$ , and  $b_n$  are the Fourier coefficients. The transient signal  $f(t)$  is sampled in  $N$  discrete equidistant times  $k\Delta t$  with the period width  $T_E = N\Delta t$ ; where  $k = 0$  to  $N-1$ , and  $\Delta t$  denotes the sampling interval. The

transient sampling process ( $t = 0$ ) starts immediately after the end of the delay time  $t_0$  (recovery time). Note that, the DLTFs system must consider a delay time ( $t_0$ ) before recording the transient data to eliminate the pulse overload recovery of the capacitance meter or current amplifier after the end of the filling pulse, as shown in Fig. 2(b). After that ( $t = 0^+$ ), the entire transient undergoes the Fourier transform analysis, contrary to the conventional boxcar and lock-in procedures where only a part of the transient is investigated. The emission transient obeying the real exponential function is represented as follows [17,18]:

$$f(t) = A \exp(-(t+t_0)/\tau_e) + B \quad (7)$$

where  $A$  and  $B$  are the amplitude and offset of the transient, and  $\tau_e$  is the emission time constant. The Fourier coefficients for the real exponential function are given based on the work of Weiss *et al.* [12]

$$a_0 = \frac{2A}{T_E} \exp(-t_0/\tau_e) [1 - \exp(-T_E/\tau_e)] \tau_e + 2B \quad (8)$$

$$a_n = \frac{2A}{T_E} \exp(-t_0/\tau_e) [1 - \exp(-T_E/\tau_e)] \frac{1/\tau_e}{1/\tau_e^2 + n^2\omega^2} \quad (9)$$

$$b_n = \frac{2A}{T_E} \exp(-t_0/\tau_e) [1 - \exp(-T_E/\tau_e)] \frac{n\omega}{1/\tau_e^2 + n^2\omega^2} \quad (10)$$

The emission time constant ( $\tau_e$ ) can be determined from the ratio of Fourier coefficients in three different ways [7,17,18]:

$$\tau_e(a_n, a_k) = \frac{1}{\omega} \sqrt{\frac{a_n - a_k}{k^2 a_k - n^2 a_n}} \quad (11)$$

$$\tau_e(b_n, b_k) = \frac{1}{\omega} \sqrt{\frac{kb_n - nb_k}{k^2 nb_k - n^2 kb_n}} \quad (12)$$

$$\tau_e(a_n, b_n) = \frac{1}{n\omega} \frac{b_n}{a_n} \quad (13)$$

In this way, the time constant of each transient is directly extracted during the thermal scan, so it is referred to as the direct evaluation method (not by indirect means such as evaluating the peak maximum temperature). Since the ratio of Fourier coefficients in Eqns. 11-13 is used (rather than inspecting the amplitude or offset), the temperature dependence of the signal magnitude may not induce an error in the emission time constant computation. If a particular range of time constants follows the typical Arrhenius temperature behaviour, those ( $\tau_e, T$ ) pairs can be used to identify the trap activation energy from the Arrhenius plot. It is essential to check whether the acquired transient is exponential or not, else it may cause systematic errors in the results. The transient should satisfy the following criteria to become an exponential class (tau-class) [7,17,18]:

$$a_2 < a_1 < 4a_2 \quad (15a)$$

$$b_2/2 < b_1 < 2b_2 \quad (15b)$$

$$\frac{b_1}{a_1} \frac{a_2}{b_2} = \frac{1}{2} \quad (15c)$$

The DLTFs software module internally computes tau-class for the measured transients during the thermal scan as per the Eqns. 15(a)-(c). Only tau-class above 60 ( $\tau_{\text{class}} > 60$ ) is selected for the direct evaluation procedure, and the remaining non-exponential transients ( $\tau_{\text{class}} < 60$ ) are rejected by the software. Since the real exponential transients are accepted for further analysis, it is possible to separate the overlapping emission transients in the DLTFs spectra.

The amplitude ( $A$ ) is estimated by extrapolating the transient signal at  $t = 0$  (immediately after  $t_0$ ) using Eqns. 9 and 10, which can be used to estimate the net trap density in the SBD [7,17,18]

$$A = \Delta C = \frac{T_E}{2} b_n \frac{\exp(t_0 / \tau_e)}{[1 - \exp(-T_E / \tau_e)]} \frac{1 / \tau_e^2 + n^2 \omega^2}{n \omega} \quad (14)$$

In C-DLTFs,  $A$  represents the amplitude of the capacitance transient ( $\Delta C$ ). Since each Fourier coefficient carries the information of emission time constant and amplitude of the transient [17,18], only one thermal scan is sufficient to identify the activation energy ( $E_T$ ), capture cross-section ( $\sigma$ ), and trap concentration ( $N_T$ ).

### 3. Experiment

#### 3.1. Vertical GaN SBD Details

The homoepitaxial GaN growth and the SBD fabrication process steps are given elsewhere [1,3,27]. The epilayer structure consists of 5  $\mu\text{m}$  thick lightly doped  $n^-$  GaN epilayer (with Si doping concentration of  $\sim 2 \times 10^{16} \text{ cm}^{-3}$ ) grown on a highly doped  $n^+$  ( $2 \times 10^{18} \text{ cm}^{-3}$ ) free-standing GaN substrate. Ni/Au (40 nm/200 nm) metal stack was considered for the top Schottky contact with a circular pattern. Ti/Al/Ni/Au (30nm/180nm/40nm/200nm) metal stack was used to create Ohmic contact on the entire backside of the sample. The mesa etching with 400 nm depth was employed to isolate the diodes in the processed sample. The active area of the SBD is  $3.14 \times 10^{-4} \text{ cm}^2$ .

#### 3.2. DLTFs Characterization

Figure 3 shows the schematic view of the measurement setup for capacitance- and current-mode DLTFs (C-DLTFs and I-DLTFs). The device-under-test (DUT) was attached to a ceramic substrate mounted on the Janis cryostat sample stage. The DUT electrical connections were made by using soldering wire for capacitance/current measurements. The sample stage temperature was controlled by Lakeshore 336 temperature controller. As shown in Fig. 2(a), the DUT was kept under quiescent reverse bias voltage ( $V_{\text{QR}}$ ) before the filling pulse. The reduced reverse bias pulsing method (from  $V_{\text{QR}} = -5 \text{ V}$  to  $V_{\text{P}} = -0.1 \text{ V}$  for a pulse width of 100  $\mu\text{s}$ ) was employed to populate the traps in the DUT. After the end of the filling pulse, the bias voltage was reverted to the quiescent reverse bias ( $V_{\text{QR}}$ ), and the emission transient was measured for two different durations  $T_{E1} = 20.48 \text{ ms}$  and  $T_{E2} = 2.048 \text{ s}$ . The Boonton 7200 capacitance meter was used for the capacitance transient measurements at a high signal

frequency of 1 MHz. The Keysight 33500B waveform generator's voltage pulses were fed through the Boonton capacitance meter to the DUT. While the transimpedance current amplifier was utilized to record the current transients. Note that the capacitance bridge was internally disconnected automatically during the current-mode DLTFs characterization [18]. The analog output voltage of the capacitance meter was amplified and digitized by the digital data acquisition system, which comprises amplifier, anti-aliasing filter, and transient recorder. To improve the signal-to-noise (SNR) ratio, transients were repeatedly acquired and averaged until the total measurement time was reached. To synchronize the voltage pulsing operation with the transient acquisition, the waveform generator's trigger signal was given to the transient recorder. Finally, the transient data analysis (computing discrete Fourier coefficients for the transient) was performed by the PhysTech FT1030 DLTFs software.

Prior to the DLTFs experiments, the DUT was cooled to a low temperature of  $\sim 25$  K. Then the sample temperature was increased, and the transients were measured in regular temperature intervals during the thermal ramp-up scan (25 K to 460 K). The DLTFs software calculates 28 different correlation functions for every transients [18], and each Fourier coefficient carries the information of the complete transient, thus a single thermal scan is sufficient to extract the emission time constant of the transient from the available 28 data pairs  $(\tau_e, T)$ . Among the Fourier coefficients, the first-order Fourier sine coefficient  $b_1$  is used to represent the DLTFs signal [7,18].

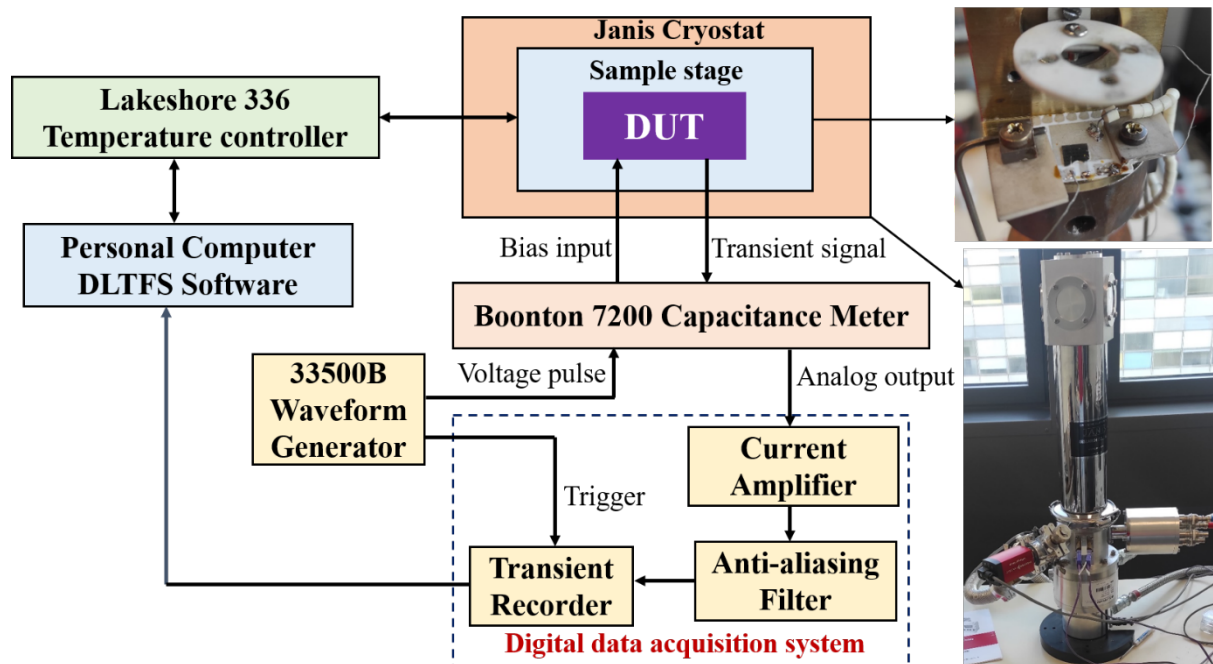


Fig. 3. Schematic view of the capacitance- and current-mode DLTFs measurement setup.

Thermally stimulated capacitance (TSCAP) spectroscopy [25] experiments were conducted to complement the DLTFs results. After the sample cooling step (device under reverse bias), the electron traps were filled by zero-biasing the diode at 25K ( $T_0$ ). Subsequently, the sample temperature was increased at a constant heating rate, and the capacitance versus temperature plot (known as TSCAP

spectrum) was measured at a constant reverse bias voltage of -5 V. The TSCAP technique is referred to as the equilibrium thermal scan at the fixed reverse bias. The TSCAP characterizations were also conducted without the trap-filling step to identify the carrier freeze-out temperature in the GaN material.

Isothermal transient spectroscopy (ITS) [18] measurements were carried out to investigate the emission and capture dynamics of the traps. Temperature stabilization (< 0.1 K) is crucial in performing reliable ITS measurements. The emission kinetics and trap activation energy were evaluated by conducting ITS at different temperatures. The capture time constant of the trap was estimated from the isothermal transients attained with shorter filling pulse widths (< 100 ns). Therefore, the trap characterization capabilities of the DLTFs technique are fully explored in the temperature range of 25K to 460 K.

## 4. Results and Discussion

### 4.1. DLTFs Results

Figure 4 shows the capacitance-DLTFs (C-DLTFs) spectra acquired with two emission transients  $T_{E1} = 20.48$  ms and  $T_{E2} = 2.048$  s for the vertical GaN-on-GaN SBDs. Two distinct peaks at ~158 K (T1) and ~320 K (T2) are noticed in the C-DLTFs for  $T_{E1} = 20.48$  ms. It is found that the emission time constants of the traps T1 and T2 follow the typical Arrhenius relation. The emission time constant ( $\tau_e$ ) is related to the activation energy ( $E_T$ ) as per the equation [28]

$$\ln(\tau_e T^2) = \frac{E_T}{kT} - \ln\left(\frac{\sigma_n N_C v_{th}}{gT^2}\right) \quad (15)$$

The Arrhenius plot  $\ln(\tau_e T^2)$  versus  $1/kT$  for the traps T1 and T2 are displayed in Fig. 5. The activation energy and capture cross-section for T1 ( $E_{T1} = 0.17$  eV,  $\sigma_{T1} = 1.1 \times 10^{-18}$  cm<sup>2</sup>) and T2 ( $E_{T2} = 0.56$  eV,  $\sigma_{T2} = 1.2 \times 10^{-15}$  cm<sup>2</sup>) are determined from the slope and intercept of the Arrhenius plot (for  $T_{E1}$ ) using the Eqn. 15. Note that, the C-DLTS techniques can discriminate the electron and hole traps in the SBD by observing the signal sign. In our measurement setup [18], positive peaks in the C-DLTFs correspond to the electron emission process associated with the trap at  $E_C - E_T$ . Accordingly, the energetic position of the traps T1 and T2 is taken at  $E_C - 0.17$  eV and  $E_C - 0.56$  eV. Since the SBD is a majority carrier device, the minority carrier injection is almost negligible even at higher forward bias conditions [29,30]. Hence, the forward bias pulsing method is ineffective in populating the hole traps in the n-type SBDs.

Similar trap parameters T1 (0.18 eV,  $1.4 \times 10^{-18}$  cm<sup>2</sup>) and T2 (0.56 eV,  $10^{-15}$  cm<sup>2</sup>) are identified from the C-DLTFs for  $T_{E2} = 2.048$  s, but the peaks (~127 K for T1, and ~265 K for T2) are noticed at lower temperatures. During the thermal ramp-up, the carrier emission from the trap level is no longer negligible in a specific temperature range, and produces a peak in the DLTFs spectra. Moreover, the emission process critically depends on the chosen emission transient duration ( $T_E$ ) at any temperature. Upon keeping a longer emission time ( $T_{E2} > T_{E1}$ ), the same traps are identified from the DLTFs but at a low temperature, as more time is available for the thermal relaxation process [6,24]. For this reason, the traps T1 and T2 are detected at relatively lower temperatures in the DLTFs attained for the longer

$T_{E2} = 2.048$  s, compared to the shorter  $T_{E1}$ . As because  $T_E = \tau_e$  only at the maximum of the peak of each Fourier coefficient. The interest in using several  $T_E$ , is to obtain a good Arrhenius plot on a large temperature interval. The trap signature can be calculated using all points of  $T_E$ , so it should increase the precision of the DLTFs results; the same is evident from the well-aligned Arrhenius plots in Fig. 5.

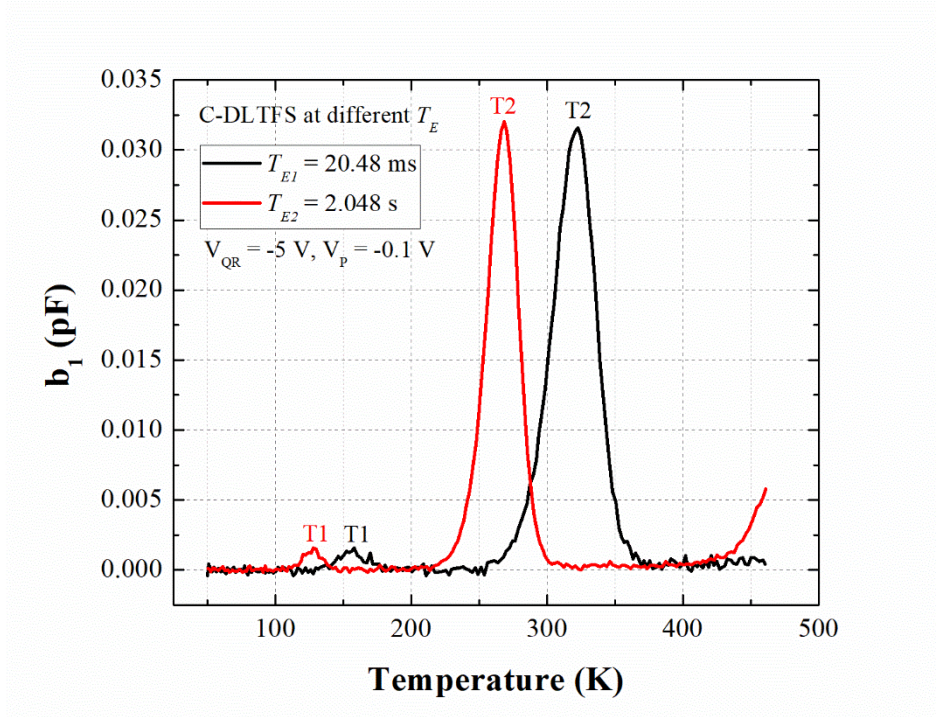


Fig. 4. C-DLTFs spectra acquired with two different emission transient times  $T_{E1} = 20.48$  ms and  $T_{E2} = 2.048$  s show two traps T1 and T2 in the vertical GaN-on-GaN SBD.

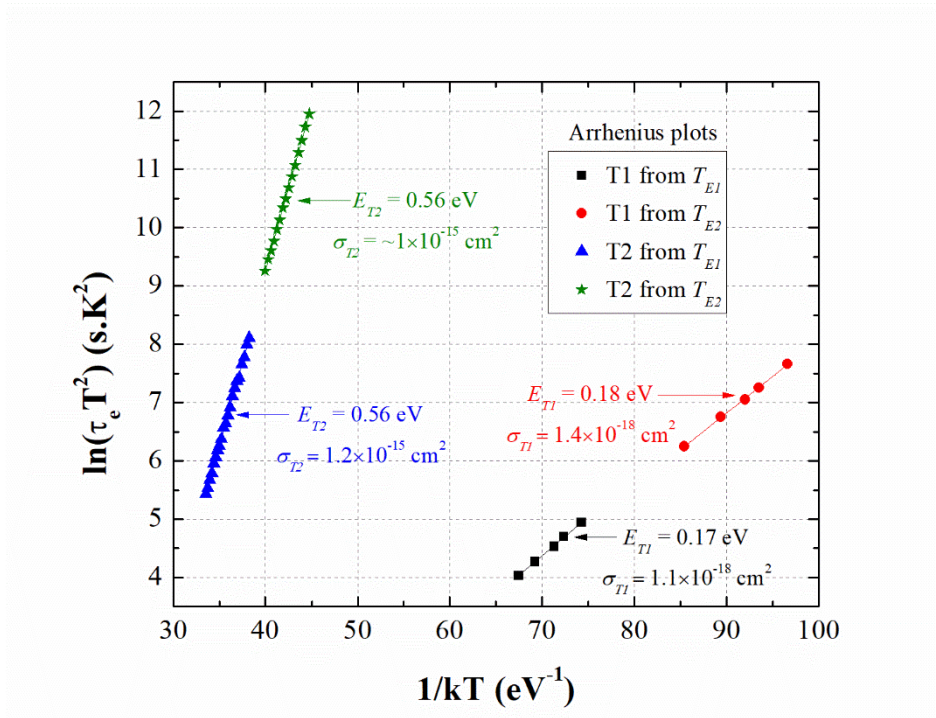


Fig. 5. Arrhenius plots for the traps T1 and T2 obtained with two different emission transients  $T_{E1} = 20.48$  ms and  $T_{E2} = 2.048$  s.

The trap density ( $N_T$ ) for T1 and T2 is computed from the DLTFs transient signal magnitude ( $\Delta C$ ) by using the following expression [7,18]

$$N_T \approx 2N_D \frac{\Delta C}{C_R} \quad (16)$$

where  $C_R$  is the quiescent reverse bias capacitance  $V_{QR} = -5$  V, and  $N_D$  is the effective doping concentration ( $2 \times 10^{16} \text{ cm}^{-3}$ ) in the GaN layer. The calculated trap concentration ( $N_T$ ) for T1 and T2 is about  $3.8 \times 10^{13} \text{ cm}^{-3}$  and  $8 \times 10^{14} \text{ cm}^{-3}$ , respectively. Because of the low  $N_T$ , a small peak is detected for T1 in the C-DLTFs spectra. The shallow trap T1 at  $E_C - 0.18$  eV is attributed to the nitrogen-vacancy ( $V_N$ ) defect [8,13]. The trap energy for the  $V_N$  defect is reported in the range of 0.18 eV to 0.25 eV [8-16]. The deep level trap T2 at  $E_C - 0.56$  eV is related to the nitrogen-antisite ( $N_{Ga}$ )-related defect observed in the n-type GaN epilayers [10,13]. In the literature, the activation energy for the trap T2 is identified from 0.53 eV to 0.61 eV [8-16]. The detected difference in the trap activation energy may be due to the variance in the epilayer doping concentration, epilayer structure, used defect characterization method, and chosen bias voltage during the emission transients. The trap concentration for T1 and T2 ( $N_{T1} = 3.8 \times 10^{13} \text{ cm}^{-3}$ , and  $N_{T2} = 8 \times 10^{14} \text{ cm}^{-3}$ ) is found to be lower in the studied GaN SBDs, compared to the  $N_T$  values ( $6.4 \times 10^{13} \text{ cm}^{-3}$ , and  $1.3 \times 10^{15} \text{ cm}^{-3}$ ) reported by Tokuda *et al.* [10]. This indicates the crystalline quality of the GaN epitaxial layer used in this work.

The current-DLTFs (I-DLTFs) spectra attained with the emission transient  $T_{EI} = 20.48$  ms are depicted in Fig. 6. The electron trap T2 at  $E_C - 0.56$  eV is identified from the I-DLTFs characteristics, while the other trap T1 is not detected. It is worth mentioning that the C-DLTFs is the more sensitive technique to characterize trap levels in junction-type devices. Unlike C-DLTS, the current transients always have the same sign as the applied electric field directing the charge flow [7,24-26], so the resultant current movement is in a unique direction. Thus, the I-DLTS measurements cannot differentiate the electron and hole traps in the SBDs. On the other hand, the I-DLTFs method [24,31] is perfectly suitable for identifying the traps in the high-resistivity crystals and heavily-irradiated samples, where it is challenging to make a rectifying junction.

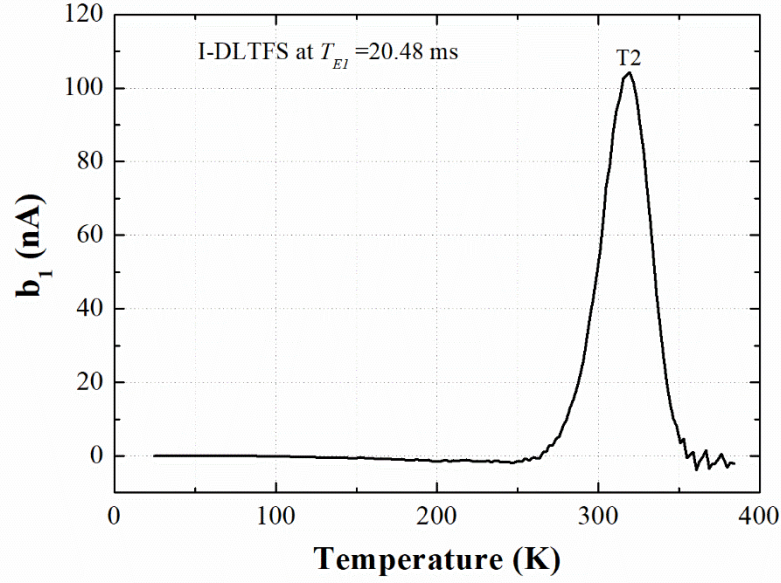


Fig. 6. I-DLTFS spectra attained with the emission transient  $T_{EI} = 20.48$  ms indicate the deep level trap T2 at  $E_C - 0.56$  eV in the vertical GaN-on-GaN SBD.

#### 4.2. TSCAP Spectroscopy

The fundamental differences between the DLTFs and the TSCAP techniques are discussed first [6,7,24-26]. In the DLTFs characterization, the emission transients (instantly after the trap-filling pulse) are repeatedly acquired in regular intervals during the thermal scan. Hence, the DLTFs results are reversible, i.e. spectra can be obtained during the thermal ramp-up and ramp-down scans. In the TSCAP, the trap-filling step is accomplished only at the low temperature (at 25 K in this work), beyond that point (no more trap-filling) merely the change in the equilibrium depletion capacitance value is measured during the temperature warm-up cycle. As a result, the TSCAP results are irreversible as the trap-filling is accomplished only at a low temperature. The DLTFs signal generation depends on the sample temperature and the selected emission transient duration, whereas the temperature solely controls the equilibrium TSCAP scan. The DLTFs technique can effectively identify the low concentration ( $N_T$ ) defects too, while the TSCAP signal sensitivity is poor for detecting the traps with  $N_T \leq 0.1 N_D$  [7,24-26]. Therefore, the DLTFs is a powerful method to characterize traps in the SBDs. However, the measurement setup for the TSCAP spectroscopy is relatively simple, relative to the DLTFs. Furthermore, the TSCAP experiments may be helpful in some aspects, such as determining the carrier freeze-out temperature in the semiconductor.

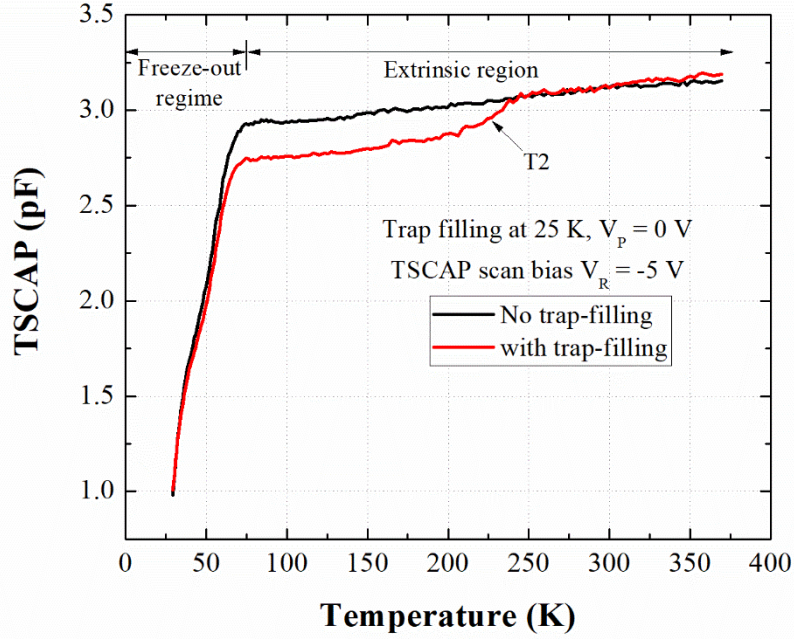


Fig. 7. TSCAP spectroscopy (trap filling at 25 K with  $V_p = 0$  V and TSCAP scan bias  $V_R = -5$  V) for the Si-doped vertical GaN-on-GaN SBD reveals the presence of trap T2 and the carrier freeze-out temperature ( $T < 75$  K) in the GaN material.

The TSCAP spectra (at  $V_R = -5$  V) for Si-doped vertical GaN-on-GaN SBD measured with and without trap-filling conditions are illustrated in Fig. 7. In the cryogenic temperature region ( $T < 75$  K), a rapid rise in the capacitance is noticed in the TSCAP spectroscopy for both conditions (even for no trap-filling case), due to the activation of donor dopant atoms in the GaN. Since the existing thermal energy within the GaN material is insufficient to ionize the donor impurities completely, the carrier density is not equal to donor doping concentration at these extremely low temperatures [29,32]. This temperature range is called the carrier freeze-out regime. As the temperature rises, the dopant ionization process increases in the semiconductor. Beyond the freeze-out temperature ( $T > 75$  K), the dopants are fully activated, and the ionized doping density is almost equal to the free carrier concentration (Extrinsic regime) [29,32]. Hence, the TSCAP measurements indicate the carrier freeze-out temperature ( $T < 75$  K) in the GaN material.

In the extrinsic region, a sharp rise in the capacitance (TSCAP step, T2) is observed in the temperature range of 205 K to 245 K. While the rising trend is absent for the no trap-filling case, signifying that the TSCAP step (T2) is induced due to the electron detrapping phenomena and is explained as follows [24,25]: Without trap-filling, the ionized donors ( $N_D^+$ ) in the SCR principally contribute to the diode depletion capacitance ( $C_R$ ). Successively after the trap-filling at 25K, captured electrons ( $n_T$ ) in the traps compensate the ionized donors, and the effective space charge density of the SBD decreases. Consequently, the depletion capacitance reduces in the extrinsic region ( $> 80$  K) as per the Eqn. (3). From a specific temperature ( $> 205$  K), the trapped electrons attain sufficient thermal

activation energy ( $E_a > E_C - E_T$ ) to overcome the potential barrier, so that the electrons are thermally emitted to the conduction band and are swept out by the electric field. This thermal-assisted electron detrapping process is seen as an increasing capacitance step in the TSCAP spectroscopy. The relation between the trap energy ( $E_T$ ) and the TSCAP mid-temperature ( $T_{1/2}$ ) is given by [24-26]

$$E_T = kT_{1/2} \ln \left[ \frac{vkT_{1/2}^2}{q(E_T + 2kT_{1/2})} \right] \quad (17)$$

In the above equation, the escape frequency factor  $\nu = \sigma_n N_C v_{th}$  is chosen based on the DLTFs results. The identical activation energy ( $\sim 0.56$  eV) and trap density ( $\sim 10^{15}$  cm<sup>-3</sup>) are identified for T2 using the Eqns. (16) and (17). So the TSCAP results are consistent with the DLTFs. Nonetheless, the DLTFs peak position and the TSCAP signal temperature cannot be compared because of the variance in the operating principle. The transients are repetitively acquired in frequent temperature intervals during the temperature cycle in the DLTFs technique (non-equilibrium measure of the diode capacitance). Whereas only change in the static capacitance is measured while increasing the temperature (equilibrium thermal scan). Another electron trap T1 at  $E_C - 0.18$  eV is not observed in TSCAP, as its trap density ( $N_{T1} = 3.8 \times 10^{13}$  cm<sup>-3</sup>) falls well below the detection limit of the TSCAP technique  $N_T \geq 0.1 N_D$  [7,24,25]. We also notice that the TSCAP technique is based on the same principle as the admittance spectroscopy measurements. The major difference is that in TSCAP, the signal frequency is fixed ( $f=1$  MHz). While in admittance spectroscopy, the frequency variation allows us to obtain an Arrhenius plot of the trap [24,26].

#### 4.3. Isothermal Transient Spectroscopy

The DLTFs results show that the electron trap T2 at  $E_C - 0.56$  eV is prominent in the vertical GaN-on-GaN SBDs. For this reason, the carrier emission and capture dynamics of the trap T2 are investigated through isothermal transient spectroscopy (ITS). The time constant of the trap T2 is inspected under systematic variation of the emission transient ( $T_E$ ) at a stable temperature; this experiment is called period scan analysis (viz.  $b_1$  vs.  $T_E$  plot, Fig. 8) [18]. In DLTFs measurements, the emission rate of the trap is changed by varying the temperature with the constant  $T_E$ . During the period scan analysis, the emission rate remains unchanged due to the stable temperature, but the duration of the emission transient period ( $T_E$ ) varies [18]. The isothermal period scan spectra measured at different temperatures (242.5 K to 301.6 K) for the trap T2 are plotted in Fig. 8. It is essential to understand how the period scan spectrum is constructed from the isothermal transients. For example, Fig. 9 displays the capacitance transients acquired with different emission transient times ( $T_E = 0.1$  s, 0.8 s, 2 s, and 20.48s) at a fixed temperature of 271 K to construct the period scan spectrum. Figures 8 and 9 reveal that the period scan signal is maximum if the emission time constant matches the chosen  $T_E$  [18]. If  $T_E$  is located outside the emission time constant, the period scan signal goes to a minimum, as demonstrated in Figs. 8 and 9(d). Note that, the peak maximum of the period scan spectrum reflects the emission time constant of the trap T2 at the particular temperature. The emission time constant of T2 is found to increase with

the temperature ( $\tau_e = 13$  s at 242.5 K, 0.57 s at 271 K, and 40 ms at 301.6 K), as noted in Fig. 8. Accordingly, the emission time constant ( $\tau_e$ ) is extracted from the temperature-dependent period scan spectra, and the corresponding Arrhenius plot is displayed in Fig. 10. The linear regression of the Arrhenius plot yields similar activation energy and capture cross-section ( $E_{T2} = E_C - 0.56$  eV,  $\sigma_{T2} = 10^{15}$  cm<sup>2</sup>) for the trap T2. Hence, it is shown that ITS can be used to determine the trap parameters [18,28].

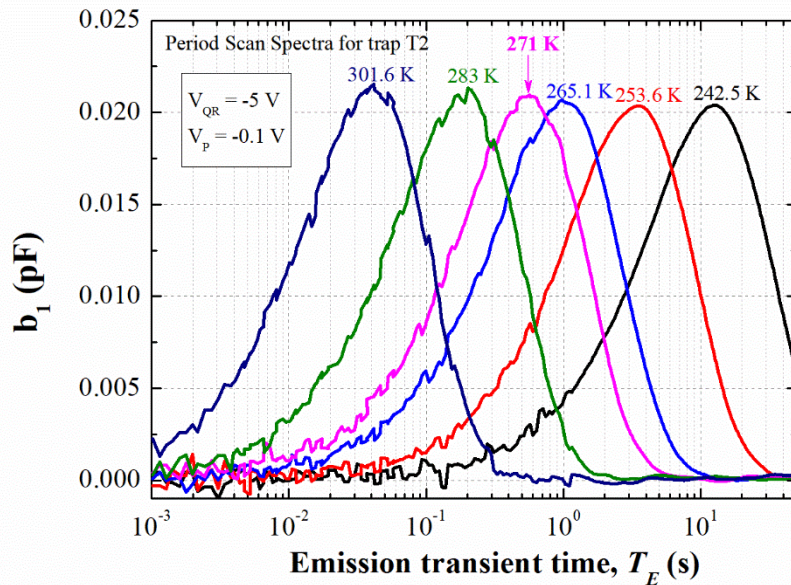


Fig. 8. The isothermal period scan spectra ( $V_{QR} = -5$  V,  $V_P = -0.1$  V) measured at different operating temperatures (242.5 K to 301.6 K) for the trap T2.

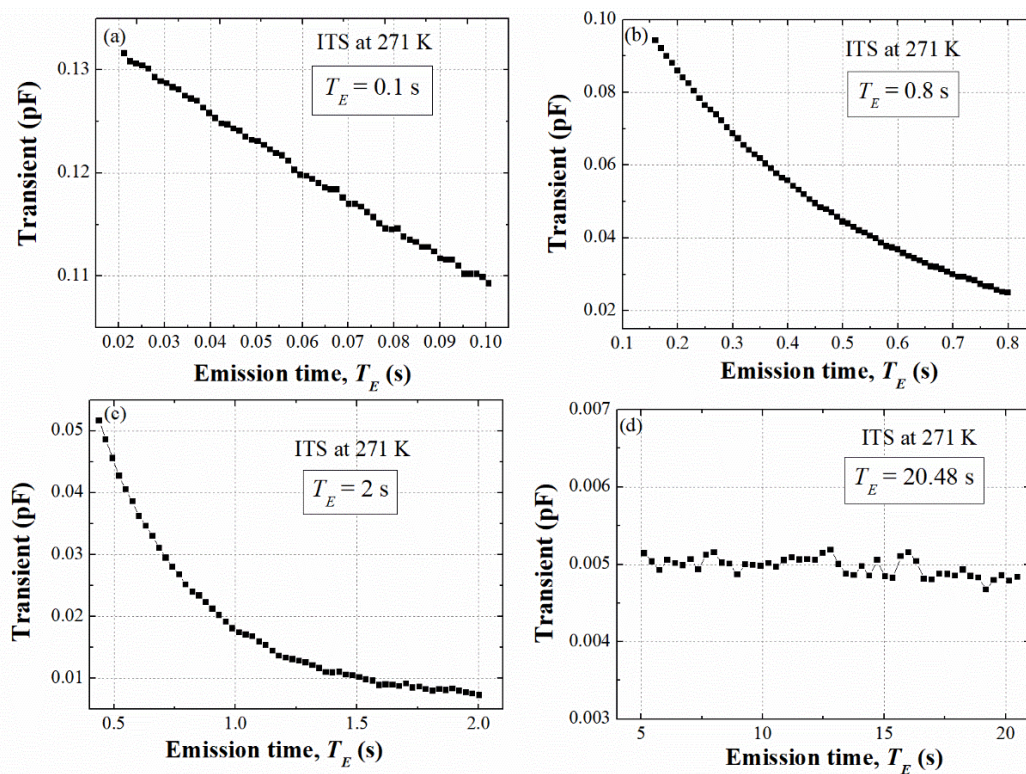


Fig. 9. The capacitance transients are acquired with different emission transient times ( $T_E = 0.1$  s, 0.8 s, 2 s and 20.48 s) at a fixed temperature of 271 K to construct the period scan spectrum.

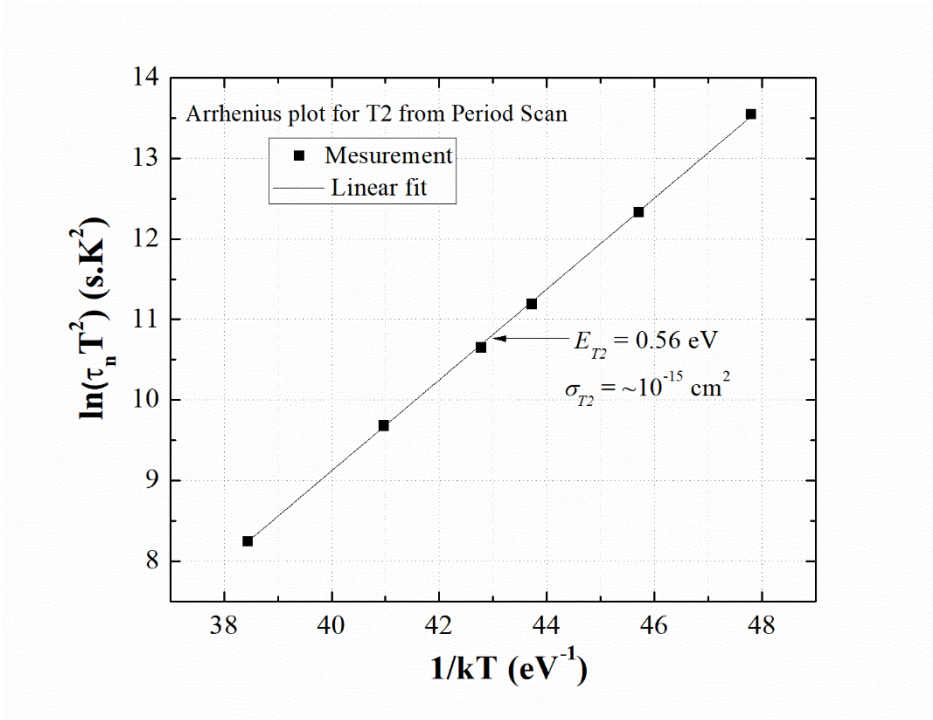


Fig. 10. Arrhenius plot for the trap T2 constructed from isothermal period scan reveal identical trap parameters.

The deconvolution analysis is carried out for the isothermal emission transients. This investigation confirms that the peak T2 arises due to the emission process from a discrete trap T2 at  $E_C - 0.56$  eV, thus no overlapping emission behaviour. The isothermal transients are further examined by varying: (a) Filling pulse voltage ( $V_P = -1$  V,  $-0.6$  V,  $-0.3$  V, and  $-0.1$  V) and (b) Quiescent reverse bias voltage ( $V_{QR} = -10$  V,  $-8$  V,  $-6$  V,  $-5$  V, and  $-4$  V). However, no considerable change in the transient amplitude ( $\Delta C$ ) is noticed upon varying these parameters, suggesting that the trap density ( $N_{T2}$ ) of T2 is uniform [18] along with the depth in the GaN active layer.

The traps are only partly filled if the filling pulse width ( $t_P$ ) is shorter than the capture time constant ( $\tau_c$ ) of the trap [6,18]. As a consequence, the resulting emission transient amplitude is smaller than expected, thereby underestimating the trap concentration ( $N_T$ ). To compute the capture time constant ( $\tau_c$ ), the isothermal emission transients are measured with the small filling pulses ( $t_P = 20$  ns to 100 ns). Figure 11 depicts the period scan spectra attained upon varying filling pulse widths ( $t_P = 20$  ns to 80 ns) at the stable temperature of 271 K. It is observed that signal magnitude upsurges with the increasing  $t_P$  (up to 70 ns), and it reaches the saturation at  $t_P = 80$  ns. This reveals that the transient amplitude depends on the filling pulse for  $t_P \leq 70$  ns. The traps (T2) are fully occupied beyond  $t_P > 80$  ns. A similar observation is noticed from the Fourier coefficient ( $b_1$ ) versus the filling pulse width plot, displayed in Fig. 12. The Fourier transform evaluation provides the capture time constant of 36 ns for the trap T2. It is worth recalling that the filling pulse width ( $t_P$ ) is chosen at 100  $\mu$ s in the DLTFs experiment; this  $t_P$  is sufficiently long enough to fill the traps in the GaN SBD completely. Therefore, our experiments

yield accurate trap concentrations for T1 at  $E_C - 0.18$  eV ( $3.8 \times 10^{13}$  cm<sup>-3</sup>) and T2 at  $E_C - 0.56$  eV ( $8 \times 10^{14}$  cm<sup>-3</sup>).

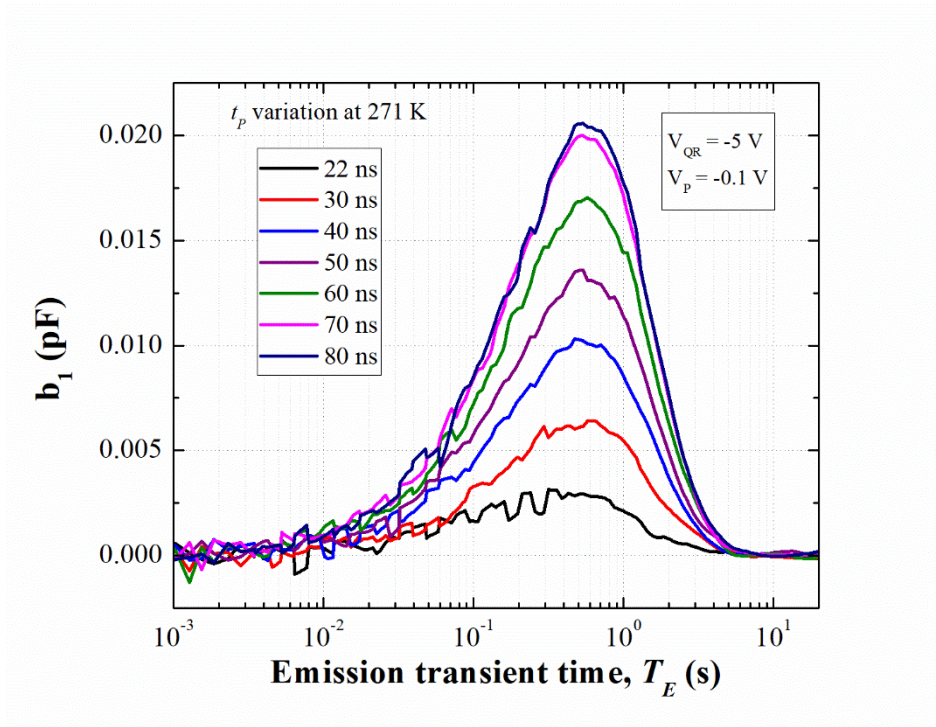


Fig. 11. Period scan spectra ( $V_{QR} = -5$  V,  $V_P = -0.1$  V) measured by varying filling pulse widths ( $t_p = 20$  ns to 80ns) at the stable temperature of 271 K.

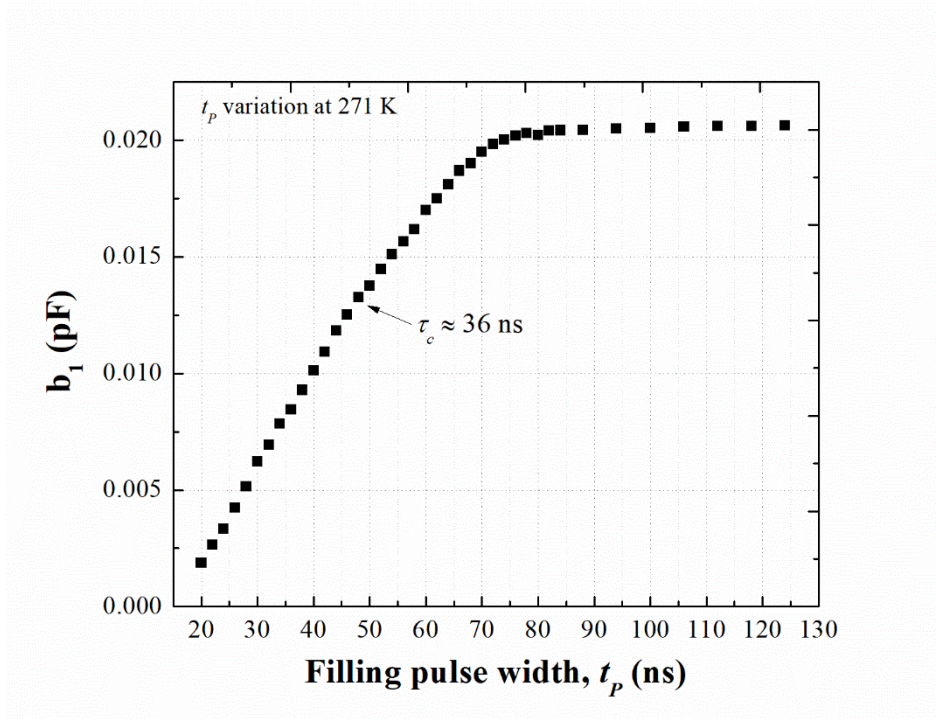


Fig. 12. Fourier coefficient ( $b_1$ ) for the emission transient is plotted with respect to change in the filling pulse width ( $t_p = 20$  ns to 130 ns).

## 5. Conclusion

The C-DLTFS characterizations reveal two electron traps T1 at  $E_C - 0.18$  eV (with  $\sigma_{n1} = \sim 10^{-18}$  cm<sup>2</sup>,  $N_{T1} = 3.8 \times 10^{13}$  cm<sup>-2</sup>) and T2 at  $E_C - 0.56$  eV ( $\sigma_{n2} = 10^{-15}$  cm<sup>2</sup>,  $N_{T2} = 8 \times 10^{14}$  cm<sup>-3</sup>) in the Si-doped vertical GaN-on-GaN SBDs. The physical origin of the traps T1 and T2 could be nitrogen vacancy ( $V_N$ ) and nitrogen antisite ( $N_{Ga}$ ), respectively. The deep level trap at  $E_C - 0.56$  eV is prominent in the studied SBDs, as found from the I-DLTS and TSCAP measurements, possibly due to its high concentration. The carrier freeze-out temperature ( $T < 75$  K) in the GaN is identified from the TSCAP spectroscopy. It is shown that the trap parameters for T2 ( $E_C - 0.56$  eV,  $\sigma_n = 10^{-15}$  cm<sup>2</sup>) are determined through the isothermal transient spectroscopy experiments. The capture time constant ( $\tau_c = 36$  ns) of the trap T2 is estimated from the isothermal transients acquired with the shorter filling pulses ( $t_P < 100$  ns). Therefore, the trap characterization capabilities of the DLTFS technique are fully explored in this study.

## Acknowledgement

The results were obtained during P. V. Raja's postdoc at Ampere Laboratory. His postdoc is financially supported by IPCEI (Important Projects of Common European Interest) on Microelectronics / Nano 2022. This project was supported by the technology facility network RENATECH and the French National Research Agency (ANR) through the project C-PI-GaN (ANR-18-CE05-0045) and the "Investissements d'Avenir" program GaNeX (ANR-11-LABX-0014). The authors would like to thank Sébastien Chenot, CNRS, CRHEA, for the support during the GaN SBD fabrication.

## References

- [1] T. H. Ngo, R. Comyn, E. Frayssinet, H. Chauveau, S. Chenot, B. Damilano, F. Tendille, B. Beaumont, J. P. Faurie, N. Nahas, Y. Cordier, Cathodoluminescence and electrical study of vertical GaN-on-GaN Schottky diodes with dislocation clusters, *J. Cryst. Growth* 552 (2020) 125911. <https://doi.org/10.1016/j.jcrysgro.2020.125911>.
- [2] L. Sang, B. Ren, M. Sumiya, M. Liao, Y. Koide, A. Tanaka, Y. Cho, Y. Harada, T. Nabatame, T. Sekiguchi, S. Usami, Initial leakage current paths in the vertical-type GaN-on-GaN Schottky barrier diodes, *Appl. Phys. Lett.* 111 (2017) 122102. <https://doi.org/10.1063/1.4994627>.
- [3] A. J. E. N'Dohi, C. Sonnevile, L. V. Phung, T. H. Ngo, P. D. Mierry, E. Frayssinet, H. Maher, J. Tasselli, K. Isoird, F. Morancho, Y. Cordier, D. Planson, Micro-Raman characterization of homo-epitaxial n doped GaN layers for vertical device applications, *AIP Adv.* 12 (2022) 025126. <https://doi.org/10.1063/5.0082860>.
- [4] F. Roccaforte, F. Giannazzo, A. Alberti, M. Spera, M. Cannas, I. Cora, B. PécZ, F. Iucolano, G. Greco, Barrier inhomogeneity in vertical Schottky diodes on free standing gallium nitride, *Mater. Sci. Semicond. Process.* 94 (2019) 164-170. <https://doi.org/10.1016/j.mssp.2019.01.036>.
- [5] D. V. Lang, Deep-level transient spectroscopy: A new method to characterize traps in semiconductors, *J. Appl. Phys.* 45 (1974) 3023-3032. <https://doi.org/10.1063/1.1663719>.
- [6] J. W. Orton, P. Blood, *The electrical characterization of semiconductors: Majority carriers and electron states*, Academic Press, London, 1992.

- [7] M. Moll, Radiation damage in silicon particle detectors - microscopic defects and macroscopic properties, PhD Dissertation, University of Hamburg, Germany, 1999.
- [8] Z.-Q. Fang, D. C. Look, P. Visconti, D.-F. Wang, C.-Z. Lu, F. Yun, H. Morkoç, S. S. Park, K. Y. Lee, Deep centers in a free-standing GaN layer, *Appl. Phys. Lett.* 78 (2001) 2178-2180. <https://doi.org/10.1063/1.1361273>.
- [9] C. B. Soh, D. Z. Chi, H. F. Lim, S. J. Chua, Comparative study of trap levels observed in undoped and Si-doped GaN, *Mat. Res. Soc. Symp. Proc.* 719 (2001) 1351-1356. <https://doi.org/10.1557/PROC-719-F13.5>.
- [10] Y. Tokuda, Y. Matsuoka, H. Ueda, O. Ishiguro, N. Soejima, T. Kachi, DLTS study of n-type GaN grown by MOCVD on GaN substrates, *Superlattices Microstruct.* 40 (2006) 268-273. <https://doi.org/10.1016/j.spmi.2006.07.025>.
- [11] Z.-Q. Fang, D. C. Look, A. Krtshil, A. Krost, F. A. Khan, I. Adesida, Giant traps on the surface of hydride vapor phase epitaxy-grown free-standing GaN, *J. Electron. Mater.* 35 (2006) 613-617. <https://doi.org/10.1007/s11664-006-0108-y>.
- [12] T. T. Duc, G. Pozina, E. Janzén, C. Hemmingsson, Investigation of deep levels in bulk GaN material grown by halide vapor phase epitaxy, *J. Appl. Phys.* 114 (2013) 153702. <https://doi.org/10.1063/1.4825052>.
- [13] P. Kamyczek, E. P.-Popko, E. Zielony, Z. Zytewicz, Deep levels in GaN studied by deep level transient spectroscopy and Laplace transform deep-level spectroscopy, *Mater. Sci.-Pol.* 31 (2013) 572-576. <https://doi.org/10.2478/s13536-013-0138-0>.
- [14] H. Yamada, H. Chonan, T. Takahashi, T. Yamada, M. Shimizu, Deep-level traps in lightly Si-doped n-GaN on free-standing m-oriented GaN substrates, *AIP Adv.* 8 (2018) 045311. <https://doi.org/10.1063/1.5011362>.
- [15] P. Kruszewski, P. Prystawko, M. Grabowski, T. Sochacki, A. Sidor, M. Bockowski, J. Jasinski, L. Lukasiak, R. Kisiel, M. Leszczynski, Electrical properties of vertical GaN Schottky diodes on Ammono-GaN substrate, *Mater. Sci. Semicond. Process.* 96 (2019) 132-136. <https://doi.org/10.1016/j.mssp.2019.02.037>. <https://doi.org/10.1063/1.1361273>.
- [16] M. Lee, C. W. Ahn, T. K. O. Vu, H. U. Lee, E. K. Kim, S. Park, First observation of electronic trap levels in freestanding GaN crystals extracted from Si substrates by hydride vapour phase epitaxy, *Sci. Rep.* 9 (2019) 1-6. <https://doi.org/10.1038/s41598-019-43583-y>.
- [17] S. Weiss, R. Kassing, Deep level transient Fourier spectroscopy (DLTFS)-A technique for the analysis of deep level properties, *Solid-State Electron.* 31 (1988) 1733-1742. [https://doi.org/10.1016/0038-1101\(88\)90071-8](https://doi.org/10.1016/0038-1101(88)90071-8).
- [18] PhysTech FT-1030 DLTFS manual, PhysTech GmbH. Am Mühlbachbogen 55d, D-85368 Moosburg, Germany, 2014.
- [19] M. Asghar, P. Muret, B. Beaumont, P. Gibart, Field dependent transformation of electron traps in GaN p-n diodes grown by metal-organic chemical vapour deposition, *Mater. Sci. Eng. B* 113 (2004) 248-252. <https://doi.org/10.1016/j.mseb.2004.09.001>.
- [20] Y. Lechaux, A. Minj, L. Méchin, H. Liang, K. Geens, M. Zhao, E. Simoen, B. Guillet, Characterization of defect states in Mg-doped GaN-on-Si p<sup>+</sup>n diodes using deep-level transient Fourier spectroscopy, *Semicond. Sci. Technol.* 36 (2020) 024002. <https://doi.org/10.1088/1361-6641/abcb19>.
- [21] K. Deng, X. Wang, S. Huang, H. Yin, J. Fan, W. Shi, F. Guo, K. Wei, Y. Zheng, J. Shi, H. Jiang, W. Wang, X. Liu, Suppression and characterization of interface states at low-pressure-chemical-vapor-deposited

- SiNx/III-nitride heterostructures, *Appl. Surf. Sci.* 542 (2021) 148530. <https://doi.org/10.1016/j.apsusc.2020.148530>.
- [22] L. Stuchlikova, J. Drobny, A. Kosa, P. Benko, A. Kopecky, S. L. Delage, J. Kovac, DLTFs study of defect distribution in InAlGaN/GaN/SiC HEMT heterostructures, in *IEEE 12th International Conference on Advanced Semiconductor Devices and Microsystems (ASDAM)* (2018) 1-4. <https://doi.org/10.1109/ASDAM.2018.8544477>.
- [23] P. Muret, C. Ulzhöfer, J. Pernot, Y. Cordier, F. Semond, C. Gacquièr, D. Théron, Electronic properties of deep defects in n-type GaN, *Superlattices Microstruct.* 3 (2004) 435-443. <https://doi.org/10.1016/j.spmi.2004.09.007>.
- [24] D. V. Lang, Space-charge spectroscopy in semiconductors, in *Thermally Stimulated Relaxation in Solids*, Springer-Verlag, Berlin Heidelberg, 1979, pp. 93-133.
- [25] P. V. Raja, N. V. L. N. Murty, Thermally stimulated capacitance in gamma irradiated epitaxial 4H-SiC Schottky barrier diodes, *J. Appl. Phys.* 123 (2018) 161536. <https://doi.org/10.1063/1.5003068>.
- [26] G. L. Miller, D. V. Lang, L. C. Kimerling, Capacitance transient spectroscopy, *Ann. Rev. Mater. Sci.* 7 (1977) 377-448. <https://doi.org/10.1146/annurev.ms.07.080177.002113>.
- [27] P. V. Raja, C. Raynaud, C. Sonnevile, A. J. E. N'Dohi, H. Morel, L. V. Phung, T. H. Ngo, P. D. Mierry, E. Frayssinet, H. Maher, J. Tasselli, K. Isoird, F. Morancho, Y. Cordier, D. Planson, Comprehensive characterization of vertical GaN-on-GaN Schottky barrier diodes, *Microelectronics J.* 128 (2022) 105575. <https://doi.org/10.1016/j.mejo.2022.105575>.
- [28] P. V. Raja, M. Bouslama, S. Sarkar, K. R. Pandurang, J.-C. Nallatamby, N. DasGupta, A. Dasgupta, Deep-level traps in AlGaIn/GaN-and AlInN/GaN-based HEMTs with different buffer doping technologies, *IEEE Trans. Electron Devices.* 67 (2020) 2304-2310. <https://doi.org/10.1109/TED.2020.2988439>.
- [29] S. M. Sze, N. N. Ng, *Physics of Semiconductor Devices*, 3rd ed., John Wiley & Sons, New Jersey, 2007.
- [30] E. H. Rhoderick, Metal-semiconductor contacts, *IEE Proc.* 129 (1982) 1-14. <https://doi.org/10.1049/ip-i-1.1982.0001>.
- [31] A. Brovko, O. Amzallag, A. Adelberg, L. Chernyak, P. V. Raja, A. Ruzin, Effects of oxygen plasma treatment on Cd<sub>1-x</sub>Zn<sub>x</sub>Te material and devices, *Nucl. Instrum. Methods Phys. Res. A* 1004 (2021) 165343. <https://doi.org/10.1016/j.nima.2021.165343>.
- [32] Simulating impurity freeze-out during low temperature operation, Simulation standard, Silvaco International, 2000. <https://silvaco.com/simulation-standard/simulating-impurity-freeze-out-during-low-temperature-operation/>.